

## REPORT

## MARTIAN GEOLOGY

## Exposed subsurface ice sheets in the Martian mid-latitudes

Colin M. Dundas,<sup>1\*</sup> Ali M. Bramson,<sup>2</sup> Lujendra Ojha,<sup>3</sup> James J. Wray,<sup>4</sup> Michael T. Mellon,<sup>5</sup> Shane Byrne,<sup>2</sup> Alfred S. McEwen,<sup>2</sup> Nathaniel E. Putzig,<sup>6</sup> Donna Viola,<sup>2</sup> Sarah Sutton,<sup>2</sup> Erin Clark,<sup>2</sup> John W. Holt<sup>7</sup>

Thick deposits cover broad regions of the Martian mid-latitudes with a smooth mantle; erosion in these regions creates scarps that expose the internal structure of the mantle. We investigated eight of these locations and found that they expose deposits of water ice that can be >100 meters thick, extending downward from depths as shallow as 1 to 2 meters below the surface. The scarps are actively retreating because of sublimation of the exposed water ice. The ice deposits likely originated as snowfall during Mars' high-obliquity periods and have now compacted into massive, fractured, and layered ice. We expect the vertical structure of Martian ice-rich deposits to preserve a record of ice deposition and past climate.

One-third of the Martian surface contains shallow ground ice. This ice is a critical target for science and exploration: it affects modern geomorphology, is expected to preserve a record of climate history, influences the planet's habitability, and may be a potential resource for future exploration. The extent of Martian ground ice and the depth to the ice table have been predicted in theory (1–3) and have been tested both in situ (4) and from orbital observations (5–11). However, the vertical structure of subsurface ice remains poorly known, including its layering, thickness, and purity, which record its emplacement and subsequent modification processes. Information about the structure, depth, and purity of shallow ice is also required to plan possible in situ resource utilization (ISRU) on future missions (12).

Early theoretical predictions suggested that Martian subsurface ice would be ice-cemented ground (2). Orbital neutron-spectrometer data have revealed ice contents greater than the likely pore space volume in the upper few centimeters of the ice table in many locations (5–7). Shallow ice (<1 to 2 m) exposed by fresh impacts remains distinct for months or years, also indicating a low rock or dust content, although possibly modified by the impact process (9, 10, 13). The Phoenix lander on the northern plains uncovered both ice-cemented regolith and deposits of pure (~99 vol-

ume %) ice (4, 14) at a few centimeters depth. The ice at that site likely extends to 9 to 66 m depth on the basis of shallow radar reflections (15), but geomorphic interpretations suggest that ice-cemented ground is dominant there (16). However, ice-loss landforms indicate that several regions on Mars have high ice volume fractions extending through substantial subsurface depths (17, 18), and radar echo power data have suggested high ice contents beneath areas of the northern plains (8). Subsurface radar reflections indicate the presence of debris-covered glaciers (19, 20) as well as buried regional ice sheets in the Utopia and Arcadia Planitiae regions that are up to 170 m thick and nearly pure ice (21, 22). Because the radar did not resolve the top of the ice, it is likely to be within ~20 m of the surface, the limit of the radar instrument's ability to iden-

tify shallow signals (15). The smaller-scale structure of the ice sheets and rocky cover are unresolvable with current radar data. It remains unknown whether the ice within a few meters of the surface has the same origin and age as the deeper ice because the upper ice is most readily modified and best coupled to the recent climate.

We describe observations of the vertical structure of ground ice using the Mars Reconnaissance Orbiter (MRO). The observations target eight locations that have steep, pole-facing scarps created by erosion (Figs. 1 and 2 and figs. S1 to S3) in images from the High-Resolution Imaging Science Experiment (HiRISE); seven are located in the southern hemisphere, and the eighth location is a cluster of scarps in Milanković Crater in the north (table S1). Each of the scarps is relatively blue (compared with surrounding terrain) in enhanced-color HiRISE images, and three locations have water-ice signatures in mid-summer spectral data (Fig. 3 and figs. S4 and S5) taken by MRO's Compact Reconnaissance Imaging Spectrometer for Mars (CRISM) (23). CRISM spectra show an H<sub>2</sub>O ice absorption feature at 1- $\mu$ m wavelength (fig. S6), which can be masked by as little as 1% soil (14). Tens of micrometers of dust are needed to make an opaque cover (24), so the dust content is low and/or wind removes dust.

Several lines of evidence indicate that the scarps are exposures of subsurface ice rather than persistent seasonal frost. First, they remain distinct from the surrounding terrain in color in all HiRISE images, including many observations acquired long after seasonal frost has sublimated from steep pole-facing slopes at higher latitudes. Second, Mars Odyssey Thermal Emission Imaging System (THEMIS) observations indicate late-afternoon scarp temperatures above the likely atmospheric frost point (23). Last, nearby pits lack relatively blue material that would be expected for topographically controlled frost (fig. S7).

The units hosting the scarps drape the terrain, with some meter-scale boulders on the surface

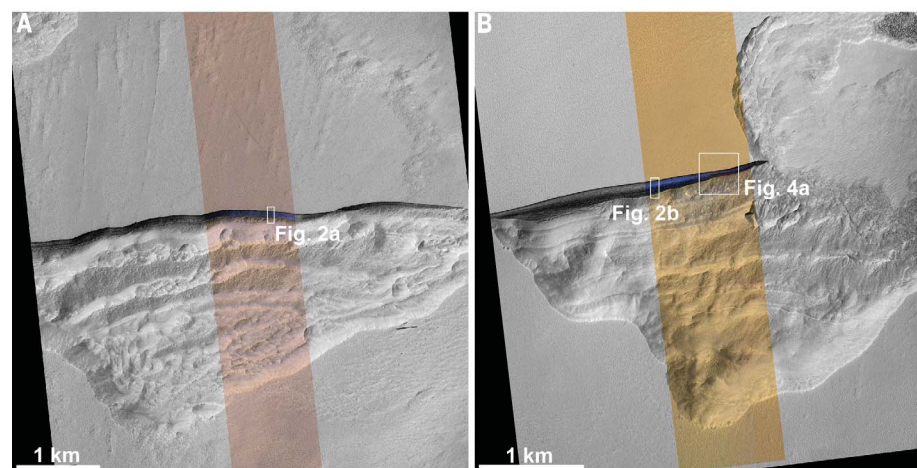


**Fig. 1. Pits with scarps exposing ice.** (A and B) Scarps 1 and 2. Both (A) and (B) show HiRISE red-filter data merged with the center color strip (23) in early-summer observations. Parallel ridges indicate retreat of scarps (fig. S1). North is up and light is from the left in all figures.

<sup>1</sup>Astrogeology Science Center, U.S. Geological Survey, 2255 N. Gemini Drive, Flagstaff, AZ 86001, USA. <sup>2</sup>Lunar and Planetary Laboratory, University of Arizona, Tucson, AZ, USA.

<sup>3</sup>Department of Earth and Planetary Sciences, The Johns Hopkins University, Baltimore, MD, USA. <sup>4</sup>School of Earth and Atmospheric Sciences, Georgia Institute of Technology, Atlanta, GA, USA. <sup>5</sup>The Johns Hopkins University/Applied Physics Laboratory, Laurel, MD, USA. <sup>6</sup>Planetary Science Institute, 1546 Cole Boulevard, Suite 120, Lakewood, CO 80401, USA. <sup>7</sup>Institute for Geophysics, Jackson School of Geosciences, University of Texas at Austin, Austin, TX 78758, USA.

\*Corresponding author. Email: cdundas@usgs.gov

and few impact craters. The surface textures show some fracturing (fig. S8), probably due to thermal contraction. Ice is expected to be stable near 10 cm depth under level ground at these locations (3). The scarps are sharply defined and nearly straight, up to ~6 km long, and face slightly east of poleward. Each scarp constitutes the equatorward side of a few-kilometer-scale pit with a rugged and sometimes boulder-rich floor, except in Milankovič Crater, where they are part of the ragged edge of a smooth plateau (fig. S2). In several cases, ridge structures parallel the scarp within the pit and merge with cusps along the margin. The base of the exposed ice appears to be covered by colluvium (Fig. 2). In several cases, surface expressions of long fractures with surrounding depressions occur on the terrain above the scarp (fig. S8).

Topographic data (figs. S9 and S10) for Scarp 1 (numbering is provided in table S1) indicates that the ice exposure has a slope of ~45° (up to 55° in some locations), transitioning to a shallower slope for the regolith-covered lower scarp. We estimate the scarp-hosting material to be at least 130 m thick after correcting for the regional slope, although the exposed ice has ≤100 m of relief because the lower slope is buried. The former value provides a better estimate of the ice-rich thickness if all of the relief is due to ice loss.

These scarps reveal the vertical structure of the ice. At several locations, ice reaches close to the top of the scarp (Fig. 2), indicating that massive ice begins at shallow depths (≤1 m). Banded patterns or variations in color or slope at some sites suggest subunits within the ice. At Scarps 6 and 7, the banded patterns show unconformities where layers cut across each other (fig. S3). The uppermost section of the scarp at each site appears steeper and less blue than the remainder. Like the Martian polar deposits (25), the color and brightness of the surface may be partially controlled by a thin coating of dust (likely a sublimation lag) and thus not representative of the bulk properties. Because lags and contaminants

will reduce the visibility of ice, it is likely that clean ice near the surface is more extensive than the limited locations where it is exposed (Fig. 2).

At Scarp 2, a lens-shaped section of the exposure lacks relatively blue coloration (Fig. 4A) and contains a concentration of boulders. Repeat images taken 3 Mars years apart show that meter-scale blocks fell from within or below this lens-shaped section (Fig. 4, B and C), providing evidence of active slope retreat. Because these blocks did not disappear after they fell [unlike ice blocks excavated by craters (10)] and originated as protrusions from the icy layer, they must be rocks that were embedded within the deposit, not chunks of ice broken off the scarp. Other sites have not shown similar blockfalls, but mottled shifts in tone and texture are common, and dark markings a few meters across appeared and disappeared at the base of some scarps (fig. S11).

The Shallow Radar (SHARAD) on MRO has detected radar contacts (reflectors) that have been interpreted as the base of ice layers in the northern plains of Mars (15, 19–22). Similar features occur near several of the scarps (fig. S12) but are difficult to distinguish from radar clutter caused by local rugged topography. Candidate reflectors in the three SHARAD tracks closest to Scarp 1 do not appear in clutter simulations by using topography derived from either Mars Orbiter Laser Altimeter (MOLA) or High-Resolution Stereo Camera (HRSC) data (23), suggesting that they could be due to the bottom of the massive ice layer. However, candidate reflectors near Scarp 5 have possible counterparts in the HRSC-based clutter simulations, suggesting that they are not subsurface features. Only these two sites have topographic data available at suitable resolution, and given the rough terrain, we cannot currently rule out unresolved clutter as the cause of candidate reflectors. Nondetections may be due to surface roughness or stratigraphic contacts that are gradual or otherwise do not produce a sharp dielectric contrast on the scale of the radar footprint.

We interpret these scarps as exposures of sub-surface ice originating as dusty snow or frost (26–29) and subsequently compacted and recrystallized. This interpretation is consistent with the high ice content and the mantling appearance of the host unit. Alternative explanations, such as growth of ice lenses (30) or enhanced vapor diffusion (31), are expected to be slow and operate at shallow depths. They should also produce layering parallel to the ground surface, unlike the layers at Scarps 6 and 7 (fig. S3). The latest ice deposition could have been geologically recent because there are few craters on the surface. The fractures and steep slopes indicate that the ice is cohesive and strong. The presence of banding and color variations suggest layers, possibly deposited with changes in the proportion of ice and dust under varying climate conditions, similar to the Martian polar-layered deposits (25). The lens-like body of lower ice content at Scarp 2 (Fig. 4A) may be a buried moraine transported by ice flow because subtle arcuate surface topography suggests glacial flow at this location (fig. S13). Alternatively, it could be a former sublimation lag; that would require some additional process to explain the presence of boulders, but some are found on the surface of the mantling deposit elsewhere (23), so this cannot be ruled out.

It is likely that the scarps are currently retreating owing to sublimation. Slope retreat caused by sublimation would explain rocks falling from Scarp 2, although the proximate cause could be seasonal frost processes or thermal cycles. Because the boulders that fell from the scarp are meter-scale, with a few percent of the boulders present having fallen over an interval of 3 Mars years, the likely retreat rate is on the order of a few millimeters each summer (unresolvable with remote imagery). This estimated retreat rate indicates that the pits may have formed over a time scale on an order of 10<sup>6</sup> years; however, the retreat rate is probably not constant. Ridges and bands paralleling the scarps may indicate former positions (Fig. 1).

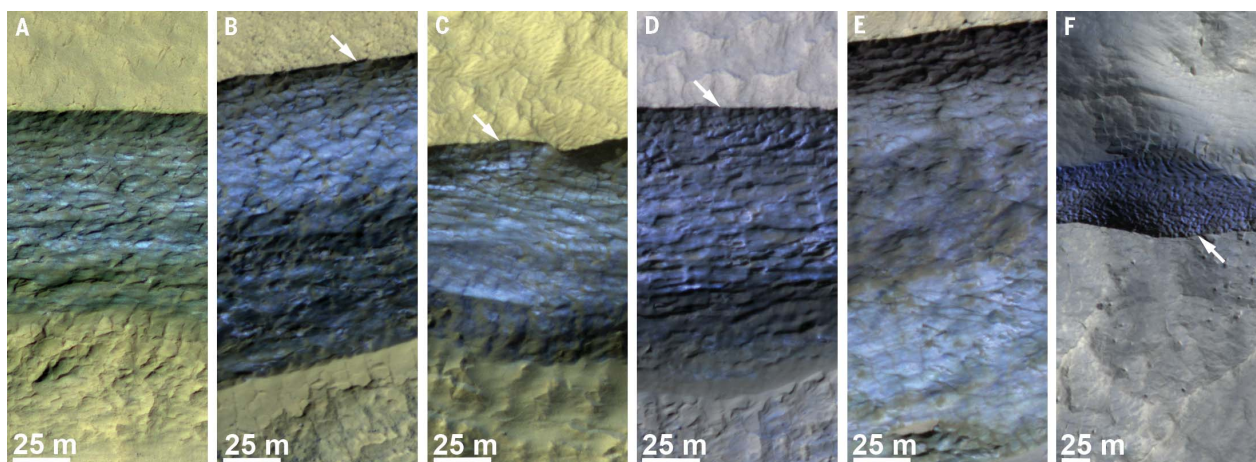


**Fig. 2. Enhanced-color transverse sections of icy scarps in late spring/early summer. (A to F)** Arrows indicate locations where relatively blue material is particularly close to the surface. Downhill is to the bottom in (A) to

(E) (Scarps 1 to 5, respectively) and to the top in (F) (Milankovič Crater). Banding or layering is visible in several scarps, and (E) shows a distinct change in color as well as multiple fractures cutting the ice.



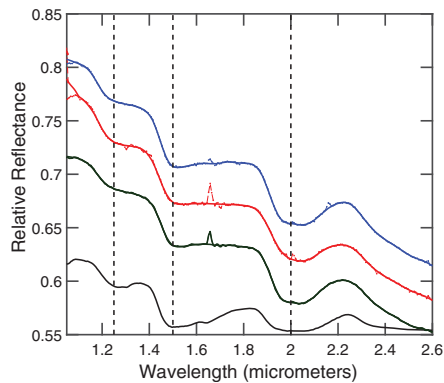


**Fig. 3. CRISM spectra of three icy scarps.** (Top to bottom lines) Scarps 2, 3, and 1 (vertically offset for clarity) compared with a laboratory water ice spectrum (32). Dashed lines indicate the centers of H<sub>2</sub>O ice absorption features. The spike near 1.65  $\mu\text{m}$  is an instrument artifact; differences in band shape are likely due to grain size (33) or minor effects of the neutral ratio region used in the CRISM spectra.

The vertical structure of the ice deposits in these exposures appears simple (fig. S14). Ice with low rock and dust content occurs at shallow depths as small as  $\sim 1$  to 2 m and extends to at least many tens of meters in depth. The ice may be capped by a cover of ice-cemented lithic material, but this veneer cannot be reliably distinguished from massive ice with a superficial lag. In some cases, the scarp color does not clearly indicate massive ice at the shallowest depths, but the textures are continuous across the ice unit. Variations in the apparent depth to massive ice could arise from both true lateral heterogeneity in ice content and from debris covering the uppermost ice, so the depth to the top of the ice sheet may be variable. Debris falling from an ice-free surface layer would be particularly effective at covering the uppermost massive ice. This simple structure matches radar interpretations of thick, regional-scale sheets of ice elsewhere on Mars, covered by lags thinner than the radar-constrained upper bound of 20 m (21, 22). Furthermore, the observations demonstrate that the massive ice in many cases occurs at depths much shallower than that upper bound. The stratigraphy indicated by the scarps may be relevant to other locations with ice-rich deposits, such as Arcadia and Utopia Planitiae. We expect that the structure at lower latitudes will be more complex (for example, more layering) or have thicker covers of ice-free and ice-cemented soil because of

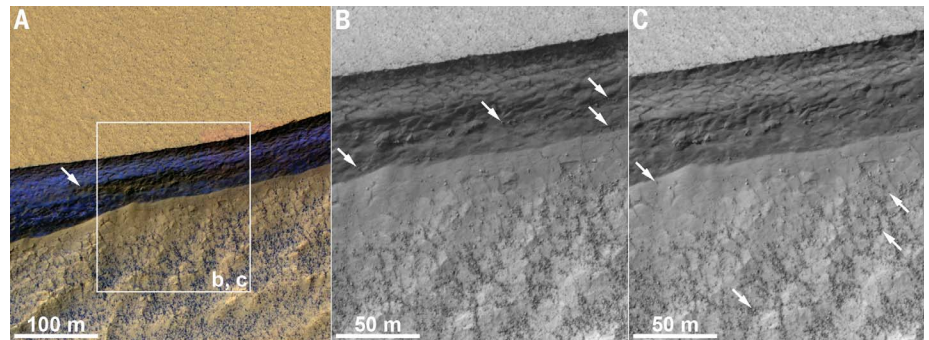


**Fig. 4. Blocks falling from an ice-rich scarp.** (A) Enhanced-color context with arrow pointing to a lens that is redder than the rest of the scarp. (B and C) Before and after images, respectively, with arrows indicating boulders that have fallen from the lens (B) to the boulder-rich pit floor (C). (B) and (C) are separated by  $\sim 3$  Mars years (table S2).

reduced overall stability and more frequent unstable conditions (28, 29).

Erosional scarps on Mars reveal the vertical structure of geologically young, ice-rich mantling deposits at mid-latitudes. The ice exposed by the scarps likely originated as snow that transformed into massive ice sheets, now preserved beneath less than 1 to 2 m of dry and ice-cemented dust or regolith near  $\pm 55^\circ$  latitude. These shallow depths make the ice sheets potentially accessible to future exploration, and the scarps present cross-sections of these ices that record past episodes of ice deposition on Mars.

#### REFERENCES AND NOTES

- R. B. Leighton, B. C. Murray, *Science* **153**, 136–144 (1966).
- M. T. Mellon, B. M. Jakosky, *J. Geophys. Res.* **98**, 3345–3364 (1993).
- M. T. Mellon, W. C. Feldman, T. H. Prettyman, *Icarus* **169**, 324–340 (2004).
- M. T. Mellon *et al.*, *J. Geophys. Res.* **114**, E00E07 (2009).
- W. V. Boynton *et al.*, *Science* **297**, 81–85 (2002).
- W. C. Feldman *et al.* in *The Martian Surface*, J. F. Bell, Ed. (Cambridge Univ. Press, 2008).
- B. Diez *et al.*, *Icarus* **196**, 409–421 (2008).
- J. Mougnot *et al.*, *Icarus* **210**, 612–625 (2010).
- S. Byrne *et al.*, *Science* **325**, 1674–1676 (2009).
- C. M. Dundas *et al.*, *J. Geophys. Res.* **119**, (2014).
- J. L. Bandfield, W. C. Feldman, *J. Geophys. Res.* **113**, E08001 (2008).
- A. Abbud-Madrid *et al.*, Report of the Mars Water In-Situ Resource Utilization (ISRU) Planning (M-WIP) study (April 2016); [https://mepag.jpl.nasa.gov/reports/Mars\\_Water\\_ISRU\\_Study.pdf](https://mepag.jpl.nasa.gov/reports/Mars_Water_ISRU_Study.pdf).
- C. M. Dundas, S. Byrne, *Icarus* **206**, 716–728 (2010).
- S. Cull *et al.*, *Geophys. Res. Lett.* **37**, L24203 (2010).
- N. E. Putzig *et al.*, *J. Geophys. Res.* **119**, (2014).
- M. T. Mellon, R. E. Arvidson, J. J. Marlow, R. J. Phillips, E. Asphaug, *J. Geophys. Res.* **113**, E00A23 (2008).
- C. M. Dundas, S. Byrne, A. S. McEwen, *Icarus* **262**, 154–169 (2015).
- S. J. Conway, M. R. Balme, *Geophys. Res. Lett.* **41**, 5402–5409 (2014).
- J. W. Holt *et al.*, *Science* **322**, 1235–1238 (2008).
- J. J. Plaut *et al.*, *Geophys. Res. Lett.* **36**, L02203 (2009).
- A. M. Bramson *et al.*, *Geophys. Res. Lett.* **42**, 6566–6574 (2015).
- C. M. Stuurman *et al.*, *Geophys. Res. Lett.* **43**, 9484–9491 (2016).
- Materials and methods are available as supplementary materials.

- E. N. Wells, J. Veveka, P. Thomas, *Icarus* **58**, 331–338 (1984).
- K. E. Herkenhoff, S. Byrne, P. S. Russell, K. E. Fishbaugh, A. S. McEwen, *Science* **317**, 1711–1715 (2007).
- J. W. Head, J. F. Mustard, M. A. Kreslavsky, R. E. Milliken, D. R. Marchant, *Nature* **426**, 797–802 (2003).
- J.-B. Madeleine *et al.*, *Icarus* **203**, 390–405 (2009).
- N. Schorghofer, *Nature* **449**, 192–194 (2007).
- N. Schorghofer, F. Forget, *Icarus* **220**, 1112–1120 (2012).
- H. G. Sizemore, A. P. Zent, A. W. Rempel, *Icarus* **251**, 191–210 (2015).
- D. A. Fisher, *Icarus* **179**, 387–397 (2005).
- R. F. Kokaly *et al.*, *USGS Spectral Library Version 7: U.S. Geological Survey Data Series 1035* 10.3133/ds1035 (2017).
- R. N. Clark, *J. Geophys. Res.* **86**, 3087–3096 (1999).

#### ACKNOWLEDGMENTS

Observation planning was funded by the MRO project, and analysis was funded by NASA grants NNH13AV851 (to C.M.D.) and NNX16AP09H (to A.M.B.). L.O. was supported by the Blaustein Postdoctoral Fellowship at Johns Hopkins University. We thank NASA/Jet Propulsion Laboratory and the instrument teams for their efforts collecting and processing data. The SHARAD instrument was provided to NASA's MRO mission by the Italian Space Agency (ASI). We thank M. Christoffersen for help with the HRSC-based clutter simulations, which are available at <https://doi.org/10.6084/m9.figshare.5537893>. The authors declare no competing financial interests. All of the primary spacecraft data used in this study are available via the Planetary Data System. HiRISE and CTX data are at <https://pds-imaging.jpl.nasa.gov/volumes/mro.html>, SHARAD data are at <http://pds-geosciences.wustl.edu/missions/mro/sharad.htm>, CRISM data are at <http://pds-geosciences.wustl.edu/missions/mro/crism.htm>, and THEMIS data and derived products are at <http://viewer.mars.asu.edu/viewer/themis#T=0>; observation ID numbers are listed in tables S2 to S5. Derived thermal inertia data are available via <https://se.psi.edu/~than/> and dust cover index and albedo via [www.mars.asu.edu/data](http://www.mars.asu.edu/data).

#### SUPPLEMENTARY MATERIALS

[www.sciencemag.org/content/359/6372/199/suppl/DC1](http://www.sciencemag.org/content/359/6372/199/suppl/DC1)  
Materials and Methods  
Supplementary Text  
Figs. S1 to S17  
Tables S1 to S5  
References (34–59)

21 June 2017; accepted 4 December 2017  
10.1126/science.aao1619

## Exposed subsurface ice sheets in the Martian mid-latitudes

Colin M. Dundas, Ali M. Bramson, Lujendra Ojha, James J. Wray, Michael T. Mellon, Shane Byrne, Alfred S. McEwen, Nathaniel E. Putzig, Donna Viola, Sarah Sutton, Erin Clark and John W. Holt

*Science* **359** (6372), 199-201.  
DOI: 10.1126/science.aao1619

### Water ice cliffs on Mars

Some locations on Mars are known to have water ice just below the surface, but how much has remained unclear. Dundas *et al.* used data from two orbiting spacecraft to examine eight locations where erosion has occurred. This revealed cliffs composed mostly of water ice, which is slowly sublimating as it is exposed to the atmosphere. The ice sheets extend from just below the surface to a depth of 100 meters or more and appear to contain distinct layers, which could preserve a record of Mars' past climate. They might even be a useful source of water for future human exploration of the red planet.

*Science*, this issue p. 199

#### ARTICLE TOOLS

<http://science.sciencemag.org/content/359/6372/199>

#### RELATED CONTENT

<http://science.sciencemag.org/content/sci/359/6372/145.full>

#### REFERENCES

This article cites 53 articles, 6 of which you can access for free  
<http://science.sciencemag.org/content/359/6372/199#BIBL>

#### PERMISSIONS

<http://www.sciencemag.org/help/reprints-and-permissions>

Use of this article is subject to the [Terms of Service](#)